AGU PUBLICATIONS

JGR

Journal of Geophysical Research: Oceans

RESEARCH ARTICLE

10.1002/2015JC011346

Key Points:
- Northwest Atlantic circulation bias is reduced in a high-resolution global climate model
- Atmospheric CO_2 doubling over 70–80 years results in an enhanced warming of the Northwest Atlantic
- The enhanced warming is associated with a weakening AMOC and regional circulation change

Supporting Information:
- Supporting Information S1
- Movie S1

Correspondence to:
V.S. Saba,
Vincent.Saba@noaa.gov

Citation:
Saba, V. S., et al. (2016), Enhanced warming of the Northwest Atlantic Ocean under climate change, *J. Geophys. Res. Oceans*, *121*, 118–132, doi:10.1002/2015JC011346.

Received 23 OCT 2015
Accepted 8 DEC 2015
Accepted article online 13 DEC 2015
Published online 8 JAN 2016

Enhanced warming of the Northwest Atlantic Ocean under climate change

Vincent S. Saba[1], Stephen M. Griffies[2], Whit G. Anderson[2], Michael Winton[2], Michael A. Alexander[3], Thomas L. Delworth[2], Jonathan A. Hare[4], Matthew J. Harrison[2], Anthony Rosati[2], Gabriel A. Vecchi[2], and Rong Zhang[2]

[1]National Oceanic and Atmospheric Administration, National Marine Fisheries Service, Northeast Fisheries Science Center, Geophysical Fluid Dynamics Laboratory, Princeton University, Princeton, New Jersey, USA, [2]National Oceanic and Atmospheric Administration, Geophysical Fluid Dynamics Laboratory, Princeton University, Princeton, New Jersey, USA, [3]National Oceanic and Atmospheric Administration, Earth System Research Laboratory, Physical Sciences Division, Boulder, Colorado, USA, [4]National Oceanic and Atmospheric Administration, National Marine Fisheries Service, Northeast Fisheries Science Center, Narragansett, Rhode Island, USA

Abstract The Intergovernmental Panel on Climate Change (IPCC) fifth assessment of projected global and regional ocean temperature change is based on global climate models that have coarse (~100 km) ocean and atmosphere resolutions. In the Northwest Atlantic, the ensemble of global climate models has a warm bias in sea surface temperature due to a misrepresentation of the Gulf Stream position; thus, existing climate change projections are based on unrealistic regional ocean circulation. Here we compare simulations and an atmospheric CO_2 doubling response from four global climate models of varying ocean and atmosphere resolution. We find that the highest resolution climate model (~10 km ocean, ~50 km atmosphere) resolves Northwest Atlantic circulation and water mass distribution most accurately. The CO_2 doubling response from this model shows that upper-ocean (0–300 m) temperature in the Northwest Atlantic Shelf warms at a rate nearly twice as fast as the coarser models and nearly three times faster than the global average. This enhanced warming is accompanied by an increase in salinity due to a change in water mass distribution that is related to a retreat of the Labrador Current and a northerly shift of the Gulf Stream. Both observations and the climate model demonstrate a robust relationship between a weakening Atlantic Meridional Overturning Circulation (AMOC) and an increase in the proportion of Warm-Temperate Slope Water entering the Northwest Atlantic Shelf. Therefore, prior climate change projections for the Northwest Atlantic may be far too conservative. These results point to the need to improve simulations of basin and regional-scale ocean circulation.

1. Introduction

The IPCC's fifth assessment of projected global and regional ocean temperature change [*Collins et al.*, 2013] is based on global climate models that have relatively coarse (~100 km) ocean and atmosphere resolutions [*Flato et al.*, 2013]. These models are sometimes too coarse to resolve regional dynamics that might affect the uncertainty of climate change projections at regional to local scales [*Stock et al.*, 2011].

In the Northwest Atlantic, particularly within the U.S. Northeast Continental Shelf, the global climate models assessed by the IPCC have a warm bias in sea surface temperature [*Wang et al.*, 2014] due to the Gulf Stream separating from the U.S. coast too far to the north of Cape Hatteras, North Carolina. Known as the "Gulf Stream separation problem" [*Dengg et al.*, 1996], this bias continues to exist in many global climate models that have an ocean component that is too coarse (~100 km) in horizontal resolution [*Bryan et al.*, 2007, and references therein]. Moreover, the coarse climate models cannot resolve the fine-scale bathymetry of the Shelf such as deep canyons, channels, and banks (i.e., Georges Bank). These topographic features impact the regional circulation of the Northwest Atlantic Shelf [*Townsend et al.*, 2006] (Figure 1). The Northwest Atlantic Ocean and Shelf is a region where colder, fresher Shelf and Slope Waters from the North (Labrador Current) converges with warmer, saltier Slope and Gulf Stream Waters from the South (Figure 1). The major throughway by which the mix of Slope Waters enters the Shelf at depth (150–200 m) is the Northeast Channel [*Mountain*, 2012] located in the Gulf of Maine (Figure 1).

To understand the impacts of climate change on the Northwest Atlantic Ocean and Shelf ecosystems, regional circulation and bathymetry in global climate models need to be improved. However, increasing the resolution of global

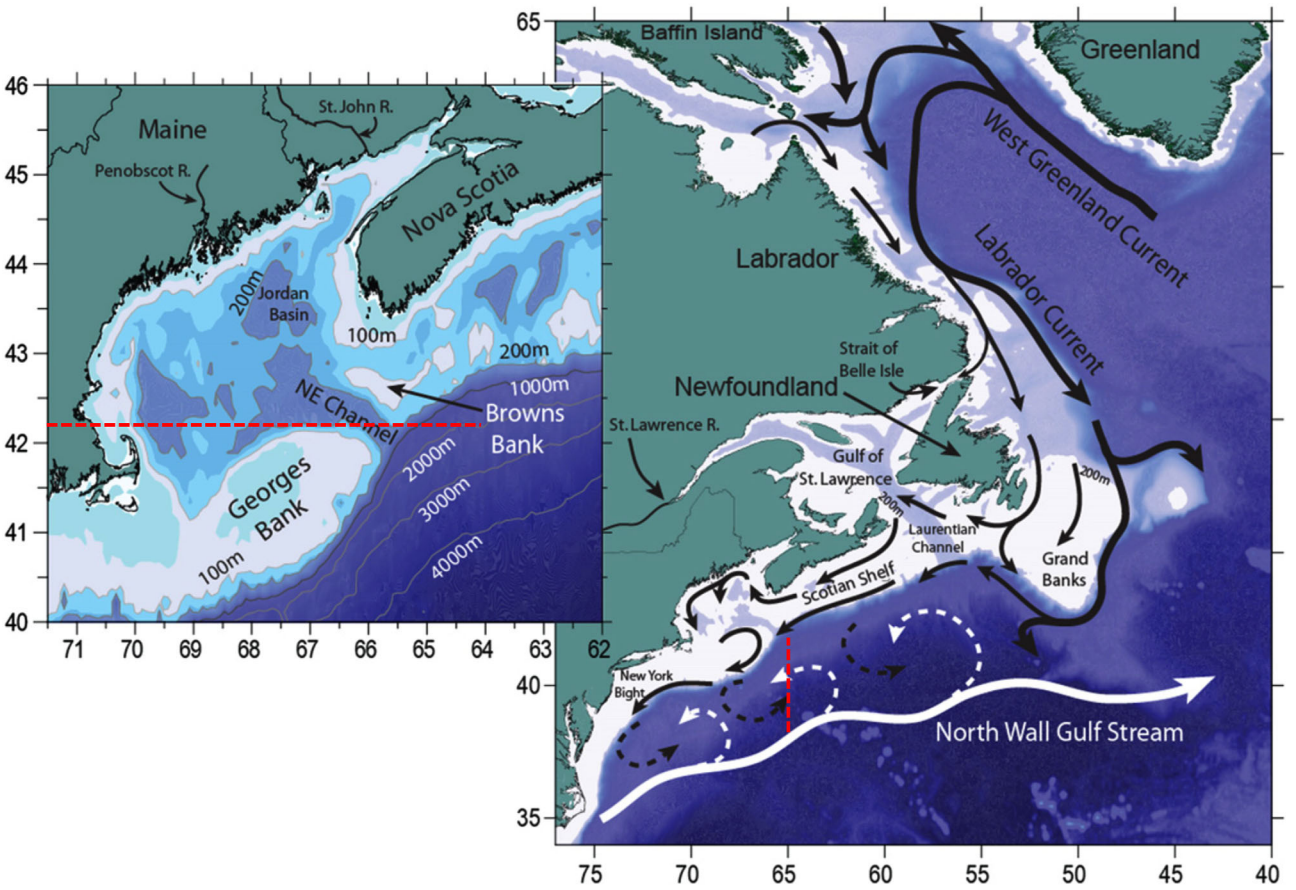

Figure 1. Northwest Atlantic Ocean and Labrador Sea bathymetry and major current systems. Black arrows are colder, fresher water associated with the Labrador Current. White arrows are warmer, saltier water associated with the Gulf Stream. Dashed arrows indicate mixing of waters (not currents) in the Slope sea. Inset shows location of the Northeast Channel (NEC; sill depth ca. 220 m) where a mix of these Slope and Shelf Waters enter the Gulf of Maine (reproduced from *Townsend et al*. [2010]). Red dashed lines represent the two transects of temperature and salinity profiles in Figures 7b and 7c.

climate models is computationally intensive [*Stock et al*., 2011] and thus only a small number of these climate models exist. Here we used a high-resolution global climate model (CM2.6) developed at the NOAA Geophysical Fluid Dynamics Laboratory (GFDL) to understand climate change impacts on the Northwest Atlantic when regional ocean circulation and bathymetry is more accurately resolved. We analyzed a hierarchy of four GFDL climate models from low resolution to high resolution (CM2.1, CM2.5-FLOR, CM2.5, CM2.6) and compared model bias relative to observed data. We also compared each model's transient climate response (atmospheric CO_2 doubling) over the course of an 80 year experimental run.

2. Models, Experiments, and Data

2.1. Global Climate Models

Details on each climate model's atmosphere/ocean horizontal and vertical resolution are in Table 1. Each climate model used in the analysis is a coupled atmosphere-ocean-land-sea ice global model. The ocean component in CM2.1 [*Delworth et al*., 2006] and CM2.5-FLOR [*Vecchi et al*., 2014] both have 1° (~100 km) average horizontal resolution but differ in their atmosphere resolution [CM2.1 = 2° (24 levels); CM2.5-FLOR = 0.5° (32 levels)]. Both CM2.5 [*Delworth et al*., 2012] and CM2.6 [*Griffies et al*., 2015; *Winton et al*., 2014] use the same atmosphere component as in CM2.5-FLOR but have higher resolution ocean components [CM2.5 = 0.25° (~25 km); CM2.6 = 0.1° (~10 km)]. Eddy parameterization is included in the ocean components of CM2.1 and CM2.5-FLOR due to the coarse grids but is absent in CM2.5 and CM2.6 [*Griffies et al*., 2015]. All ocean components have 50 vertical levels down to 5500 m.

Table 1. Details of Each GFDL Climate Model Used in the Analysis[a]

Model	Ocean Resolution (Vertical Levels)	Atmosphere Resolution (Vertical Levels)	Land Model	Sea Ice Model (Snow and Sea Ice Max. Albedos)
CM2.1	1.00° (50)	2.0° (24)	LaD	SIS (0.80 and 0.58)
CM2.5 FLOR	1.00° (50)	0.5° (32)	LM3	SIS (0.85 and 0.68)
CM2.5	0.25° (50)	0.5° (32)	LM3	SIS (0.85 and 0.68)
CM2.6	0.10° (50)	0.5° (32)	LM3	SIS (0.85 and 0.68)

[a]CM2.5 FLOR is the forecast-oriented low ocean resolution (FLOR) version of CM2.5.

2.2. Experiments

All models were initialized in the same manner such that their 1860 control simulations (global atmospheric CO_2 fixed at the year 1860 concentration) were initialized from present-day ocean conditions. The spin-up time for each model was 100 years. To calculate each model's climate change response, we used a 1%/yr increase in global atmospheric CO_2 run that went up to 80 years (CO_2 doubles at year 70) and subtracted each model's 1860 control simulation for the corresponding years or months. To account for model drift in the 1860 control simulations, we only calculated climate change differences between corresponding years or months as done in *Delworth et al.* [2012] and *Winton et al.* [2014]. We also used 1990 control simulations (global atmospheric CO_2 fixed at the year 1990 concentration) for each model to calculate biases in temperature and salinity. Further details on each model and the experiments can be found in *Delworth et al.* [2006, 2012], *Griffies et al.* [2015], *Vecchi et al.* [2014], and *Winton et al.* [2014].

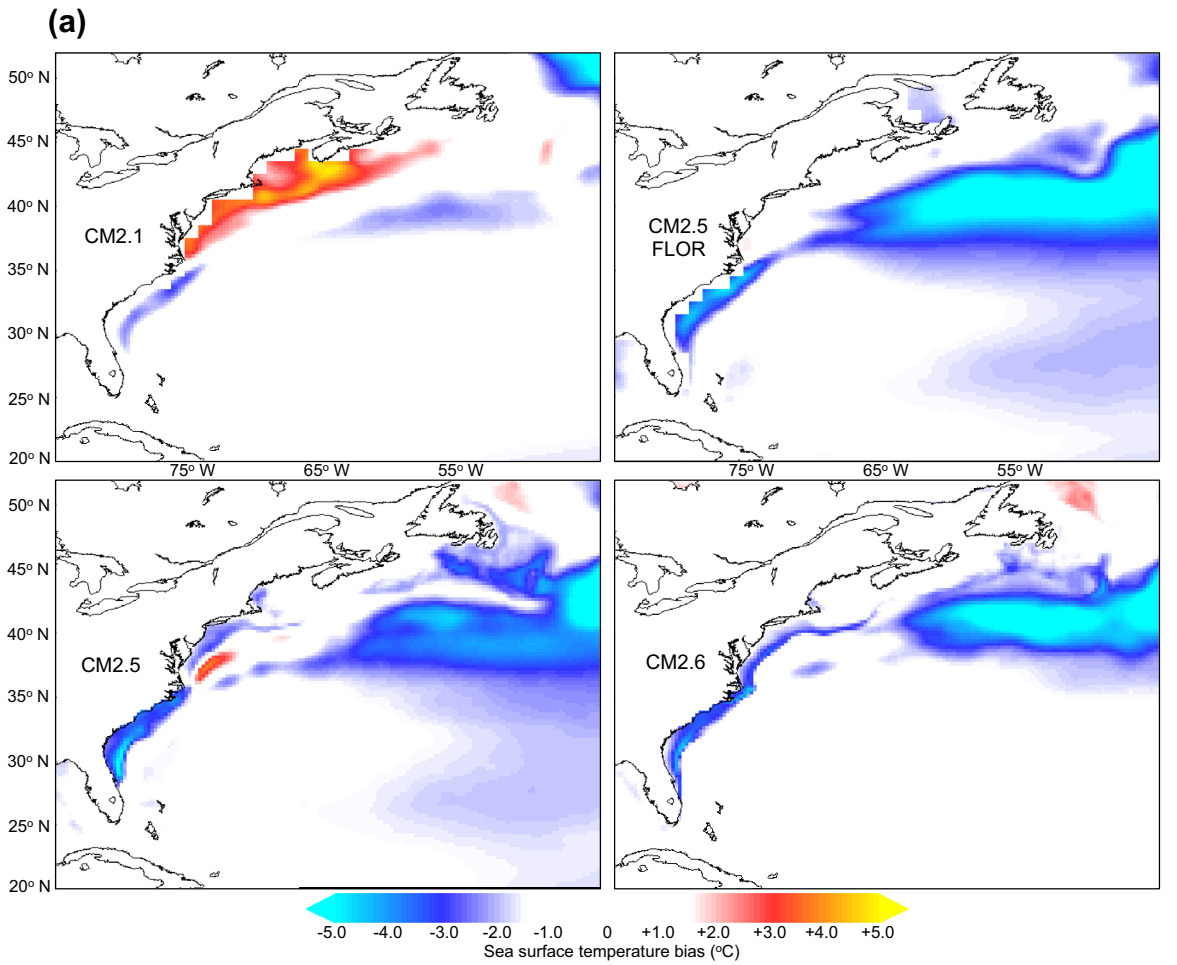

Figure 2. Modeled temperature and salinity bias in the Northwest Atlantic. (a) Sea surface temperature bias (model minus observations) of GFDL's CM2.1, CM2.5-FLOR, CM2.5, and CM2.6. Observations are based on mean NOAA OISST (Reynolds; 0.25° × 0.25°) data from 1981 to 2013. Model output is from each climate model's 1990 control simulation (40 year mean). (b) March–April surface and bottom temperature/salinity biases (model minus observations) within the U.S. Northeast Shelf. Observations are based on March–April climatologies of NOAA ship-based in situ measurements from 1977 to 2009. Model output is from each climate model's 1990 control simulation (40 year mean).

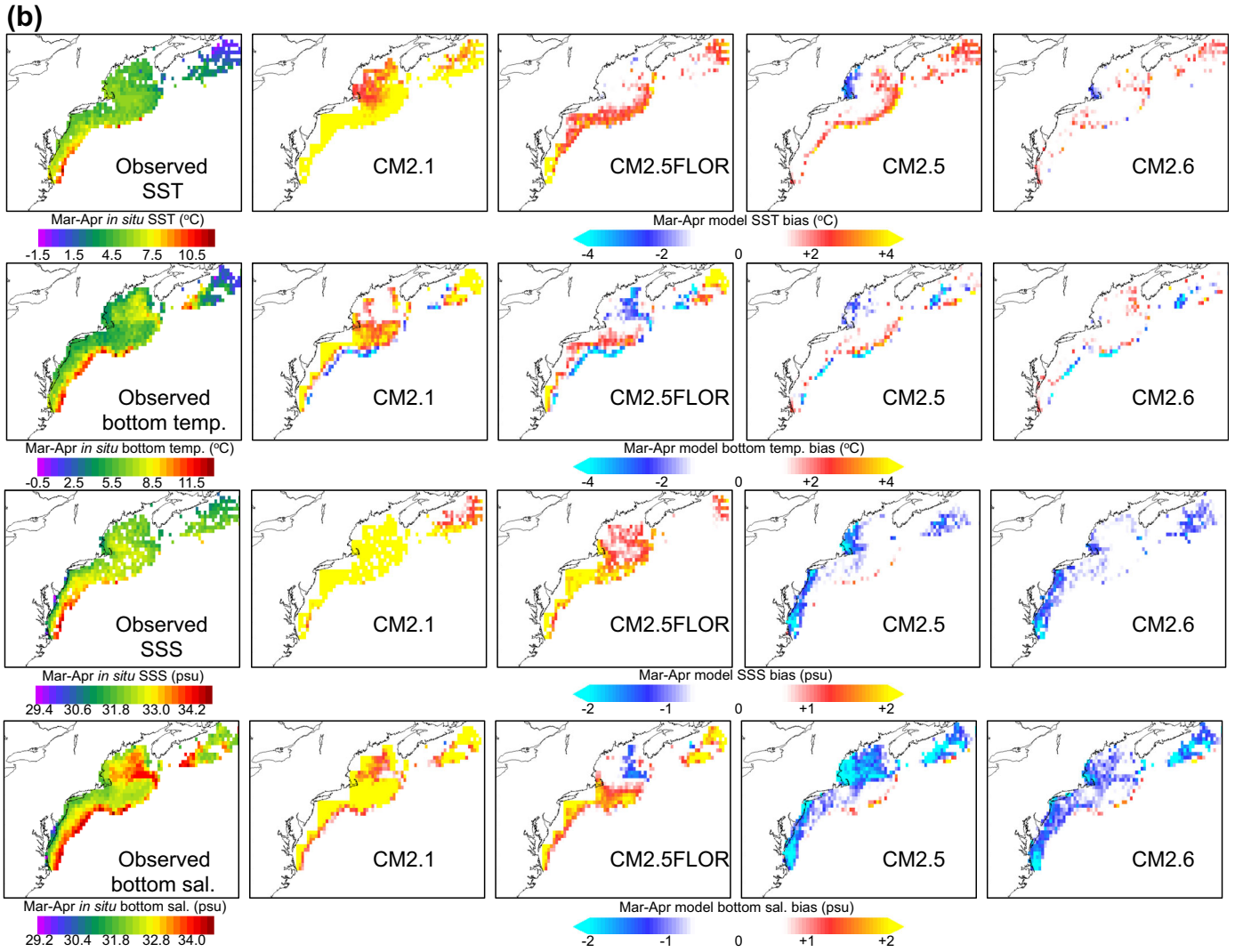

Figure 2. (Continued).

2.3. Data

We used monthly in situ temperature and salinity observations measured within the Northeast Channel [150–200 m; (polygon #29 = spatial boundaries for the Northeast Channel] from a database maintained by the Bedford Institute of Oceanography (http://www.bio.gc.ca/science/data-donnees/archive/tsc/scotia/ssmap-en.php) from 1970 to 2009. The mixing triangle boundaries in Figure 3 derive from water mass temperature and salinity observations described in *Mountain* [2012]. Observed bathymetry was from the 2014 GEBCO 30-arc sec grid (http://www.gebco.net/data_and_products/gridded_bathymetry_data/gebco_30_second_grid). Shelf and Slope Water intrusions within the Northeast Channel (Figure 3) were calculated based on methods described in *Mountain* [2012].

For sea surface temperature observations, we calculated an annual climatology using daily 0.25° NOAA OISST (Reynolds; http://www.ncdc.noaa.gov/oisst/data-access) from 1981 to 2013. In situ temperature and salinity measurements (surface and bottom) within the U.S. Northeast Shelf were used to create bimonthly 0.25° climatologies. The March–April climatology is based on a relatively large number of observations. All model biases were calculated by first regridding each climate model's ocean output to the same grid as observations.

Annual values of AMOC derived from monthly RAPID-MOC array measurements (http://www.rapid.ac.uk/rapidmoc) across the Atlantic Ocean at 26.5°N [*McCarthy et al.*, 2015]. Annual AMOC values are based on the moc_transports calculation (http://www.rapid.ac.uk/rapidmoc). The moc_transports calculation is an estimate of the meridional flow

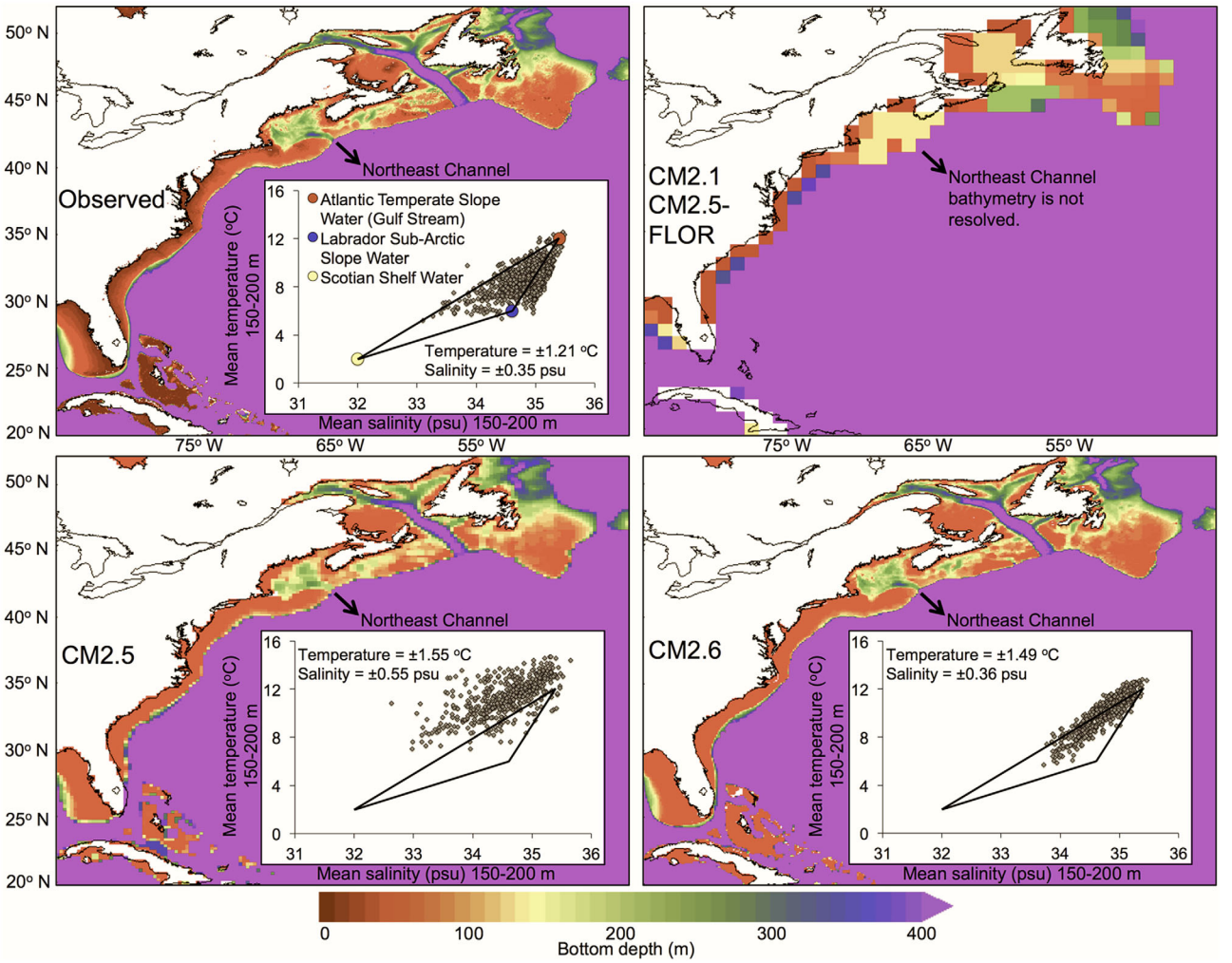

Figure 3. Observed versus modeled temperature-salinity water mass mixing triangles in the Gulf of Maine's Northeast Channel. Observed versus modeled bathymetry of the Northwest Atlantic Shelf and inset temperature-salinity water mass mixing triangles in the Northeast Channel (150–200 m). Model output derived from a 40 year period from each model's 1990 control simulation (Methods). Temperature and salinity are monthly values averaged between 150 and 200 m (grey diamonds) within the Northeast Channel (observed time period = 1970–2009, modeled = atmospheric CO_2 fixed at the year 1990 (1990 control run, 40 years)). The black mixing triangle in the three insets represents observed water mass mixing from Slope and Shelf Waters (colored circles) that enter the Northeast Channel [*Mountain*, 2012]. The standard deviation of salinity and temperature (150–200 m) are listed in each mixing triangle.

along 26.5°N, which can be obtained by decomposing it into three parts: transport through the Florida Straits, flow induced by the interaction between wind and the ocean surface (Ekman transport), and transport related to the difference in sea water density between the American and African continents (http://www.rapid.ac.uk/rapidmoc).

3. Results and Discussion

3.1. Model Bias

Bias in the coastal separation position of the Gulf Stream (warm and salty bias along Shelf) that is common to coarse models is nearly eliminated as ocean and atmosphere model resolution increases (Figures 2a and 2b). Interestingly, the annual warm bias in SST on the Shelf is in CM2.5-FLOR is eliminated (Figure 2a). This is likely due to the higher resolution of CM2.5-FLOR's atmosphere (~50 km) compared to CM2.1 (~200 km) leading to a better representation of surface wind stress. However, the warm and salty bias in the ocean surface becomes apparent in CM2.5-FLOR when it is compared to a bimonthly (March–April) in situ climatology (Figure 2b).

Both CM2.5 and CM2.6 resolve the detailed bathymetry that allows for the passage of Slope Water through the Northeast Channel and into the Northwest Atlantic Shelf system (Figure 3). In CM2.6, the modeled interannual variability of Slope Water intrusions into the Gulf of Maine is nearly identical to observations in terms

of salinity but is slightly too high in terms of temperature (Figure 3). The Northeast Channel is not resolved in the coarse models CM2.1 and CM2.5-FLOR and thus Slope Water cannot enter the Shelf at depth in these two models (Figure 3). In the intermediate resolution model (CM2.5), the Northeast Channel is resolved, although not as accurately as it is in CM2.6 (Figure 3).

Generally, CM2.6 has the least bias in global SST relative to CM2.1 and CM2.5 [*Griffies et al.*, 2015] although the North Atlantic Current in CM2.5-FLOR, CM2.5, and CM2.6 is too far to the south causing a cold bias in sea surface temperature between 35°N and 45°N (Figure 2a). This cold bias in the North Atlantic Current region is very robust and can be as high as −10°C [*Delworth et al.*, 2012]. It is suggested that this cold bias is associated with a misrepresentation of Northern overflows (refer to section 3.3), particularly in the Nordic Sea where deep water crosses through the Greenland-Iceland-Scotland ridge contributing to North Atlantic Deep Water and is part of the deep branch of AMOC [*Zhang et al.*, 2011]. However, our analysis is focused on the Northwestern region of the Gulf Stream where model bias in the coastal separation of the Gulf Stream is substantially reduced (Figure 2b).

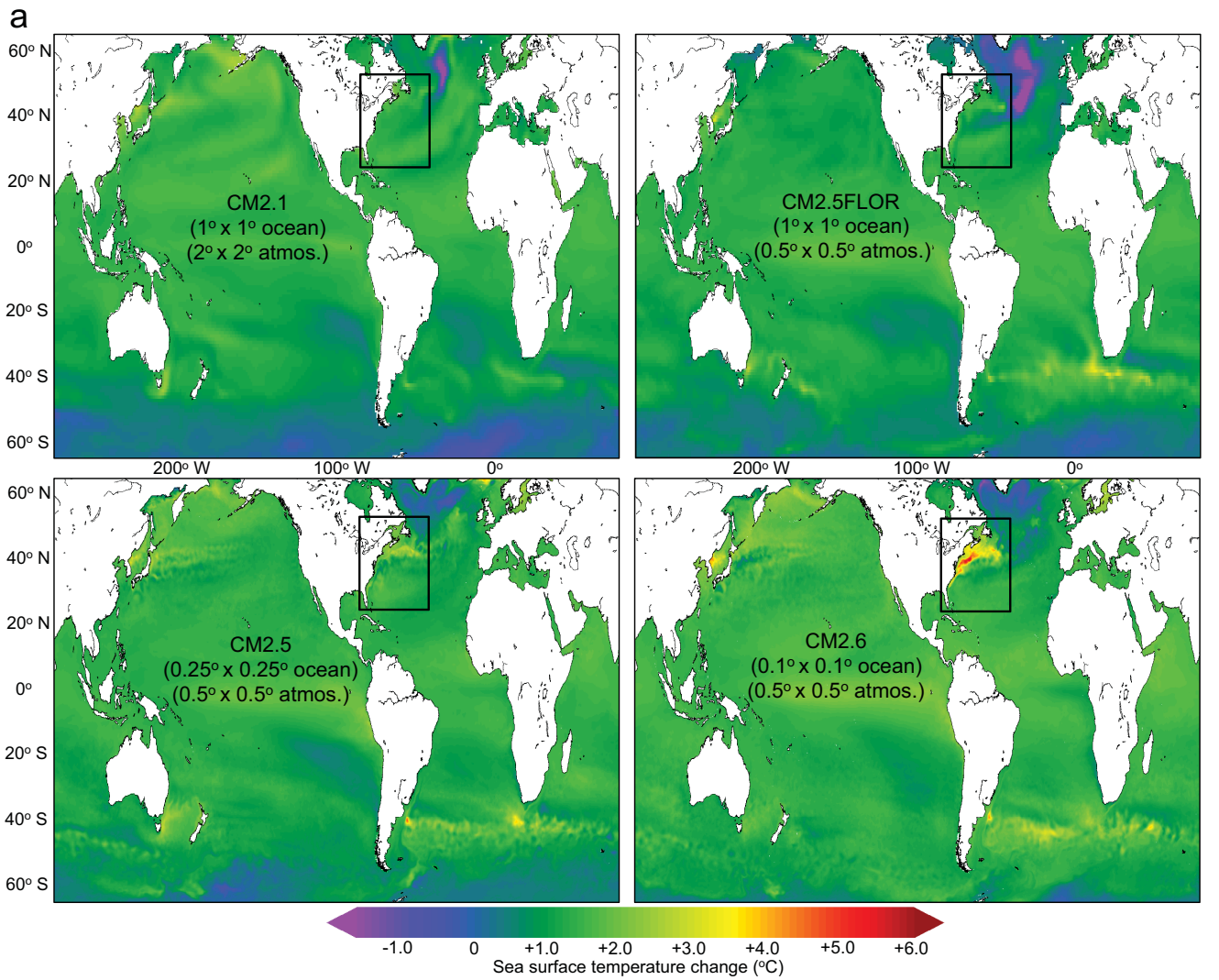

Figure 4. Global and Northwest Atlantic sea surface and upper-ocean temperature change after a doubling of global atmospheric CO_2 among four climate models of varying ocean and atmosphere resolution. In Figures 4a–4c, the CO_2 perturbation is based on a 1%/yr increase in global atmospheric CO_2 such that the concentration doubles at year 70. (a) The change in sea surface temperature (SST) is based on the difference between the mean SST from years 60 to 80 of the 2× CO_2 run and the mean SST from the corresponding 20 year period from the control run (CO_2 fixed at the year 1860 (preindustrial)). Each climate model (CM) was developed at the NOAA Geophysical Fluid Dynamics Laboratory (GFDL). Model resolutions listed in each plot are each model's global average. The black box highlights the Northwest Atlantic Ocean. (b) Northwest Atlantic (65°W to 75°W, 35°N to 45°N) upper-ocean (0–300 m) temperature change in the 80 year 2× CO_2 run among the four models. (c) Northwest Atlantic versus global upper-ocean (0–300 m) temperature change from CM2.6 in the 80 year 2× CO_2 run. In Figures 4b and 4c, ocean temperature change is smoothed by a 10 year moving average and is based on monthly differences between the 2× CO_2 run and the preindustrial control run. Refer to Table 1 for additional details of the four climate models and experiments.

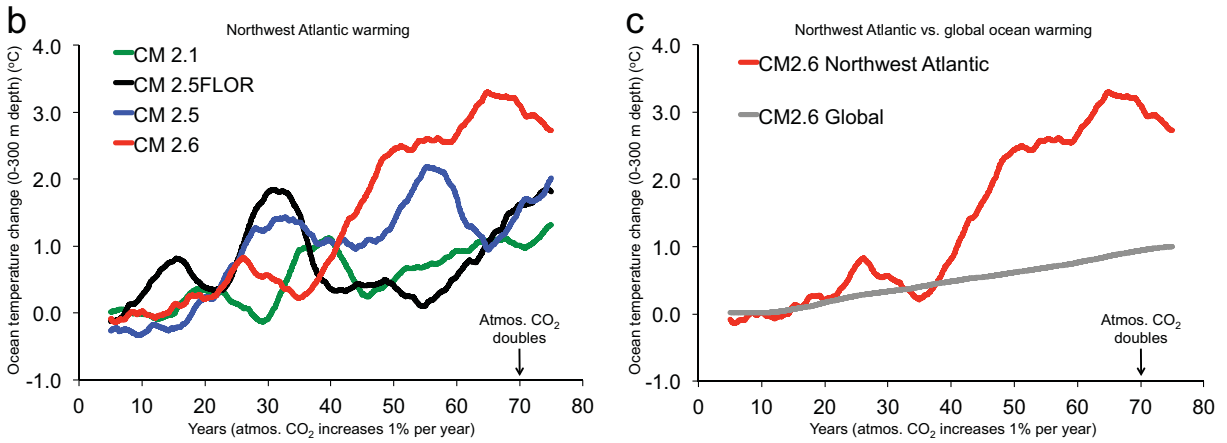

Figure 4. (continued)

3.2. Transient Climate Response

An atmospheric CO_2 doubling experiment (transient climate response) shows that there is an enhanced warming exclusive to the Northwest Atlantic Ocean in the highest-resolution global climate model CM2.6

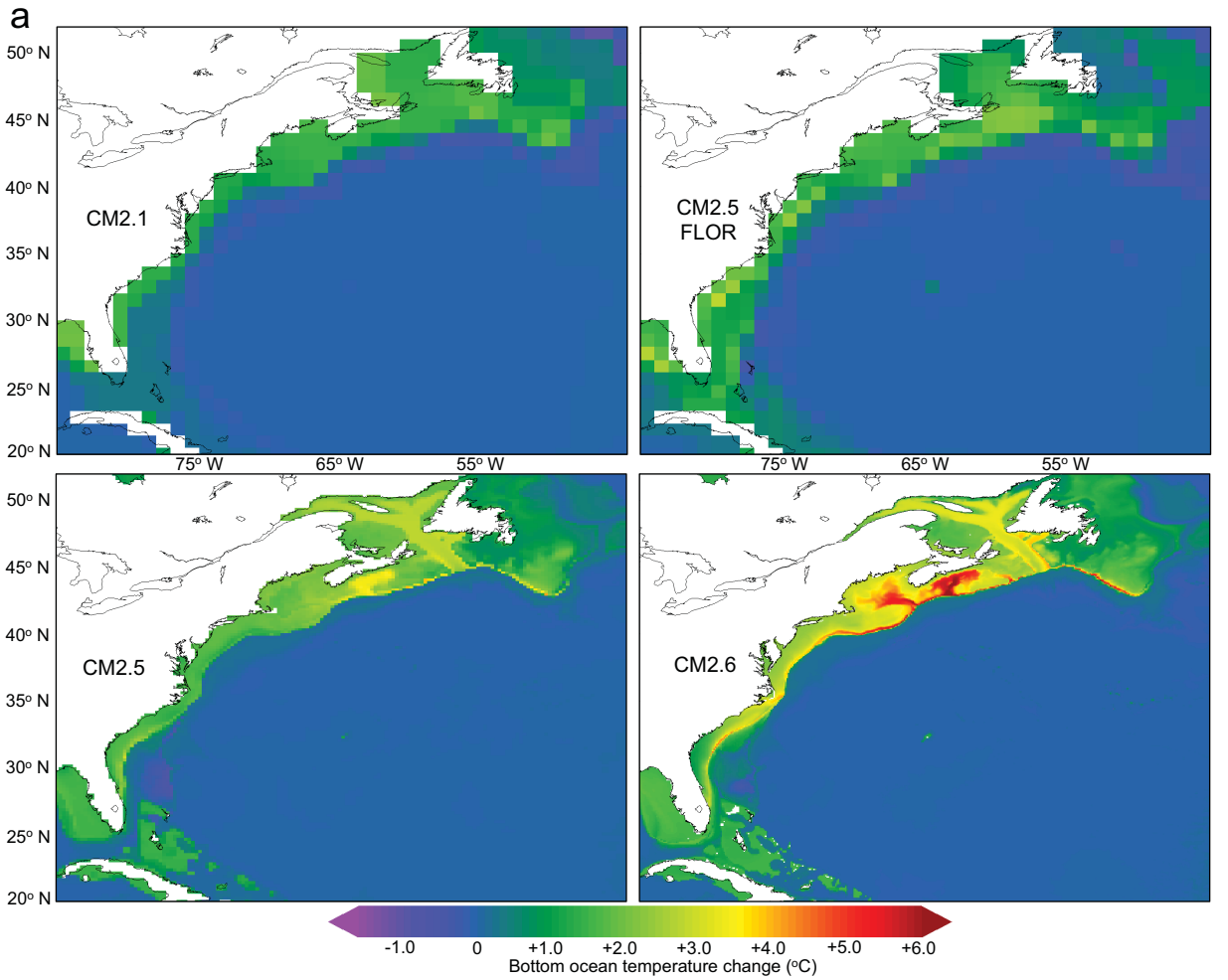

Figure 5. Northwest Atlantic Ocean and Continental Shelf change in (a) bottom temperature, (b) surface salinity, and (c) bottom salinity after a doubling of global atmospheric CO_2 among four climate models of varying ocean and atmosphere resolution. Climate model responses are based on the same experiments and time periods as in Figure 4.

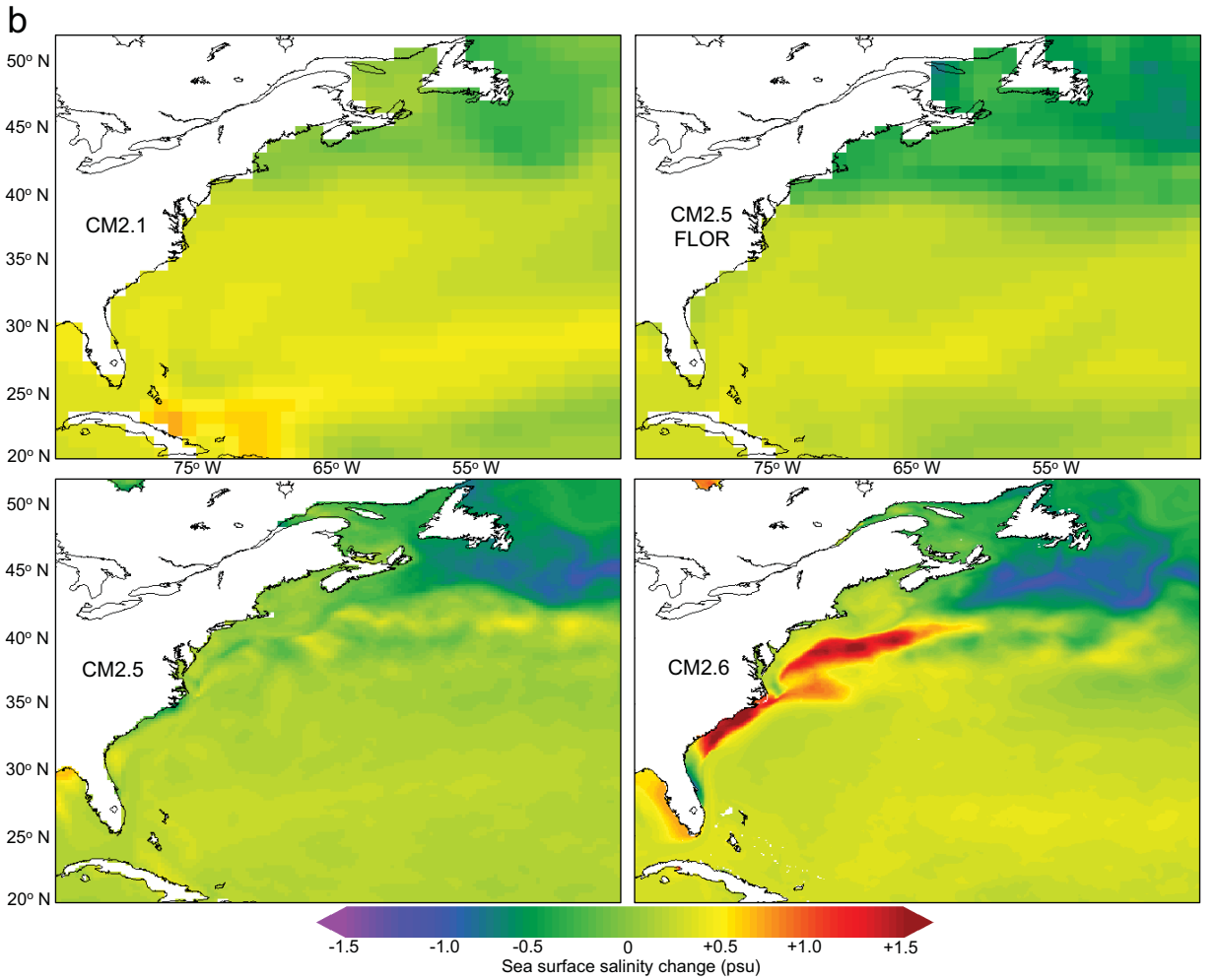

Figure 5. (continued)

(Figure 4a). The CM2.6 upper-ocean (0–300 m depth) temperature change for the Northwest Atlantic (65°W to 75°W, 35°N to 45°N) shows a warming of about 3°C after a doubling of global atmospheric CO_2 (Figure 4b), a warming rate that is two to three times faster than its global average (Figure 4c) and twice as fast as the coarsest climate model (CM2.1) (Figure 4b). The two models of intermediate resolution (CM2.5-FLOR and CM2.5) have a warming that is greater than coarsest model (CM2.1) but not nearly as high as the high-resolution model (CM2.6; Figure 4b). The CM2.6 warming for the Northwest Atlantic is about 2°C warmer compared to the coarsest climate model (CM2.1) (Figure 4b).

To understand how much of the Northwest Atlantic warming differences are attributed to natural variability versus CO_2 doubling, we examined ocean temperature variability in each climate model's control simulation that has no change in radiative forcing. Over an 80 year period (same model years in Figure 4b) in each model's control simulation, Northwest Atlantic (65°W to 75°W, 35°N to 45°N) upper-ocean (0–300 m depth) temperature varies on a decadal time-scale that is ±0.13°C (CM2.1), ±0.20°C (CM2.5), ±0.40°C (CM2.6), and ±0.48°C (CM2.5-FLOR). Therefore, the magnitude of natural decadal variability in each of these models does not exceed the difference in warming between CM2.6 and the other three models during the last 20 years of the CO_2 doubling experiment (Figure 4b).

The cooling of the subpolar North Atlantic (40°N to 60°N) occurs in all four models but varies in magnitude (Figure 4a). As shown in *Winton et al.* [2014], these differences are a function of each model's Atlantic Meridional Overturning Circulation (AMOC) weakening rate under a transient climate response such that those models with the most pronounced AMOC weakening (i.e., CM2.5-FLOR) also have the most pronounced cooling of the subpolar North Atlantic. Moreover, *Winton et al.* [2014] associated the enhanced warming of the Southern Ocean in CM2.6 (Figure 4a) with subsurface heat storage differences (vertical transport below

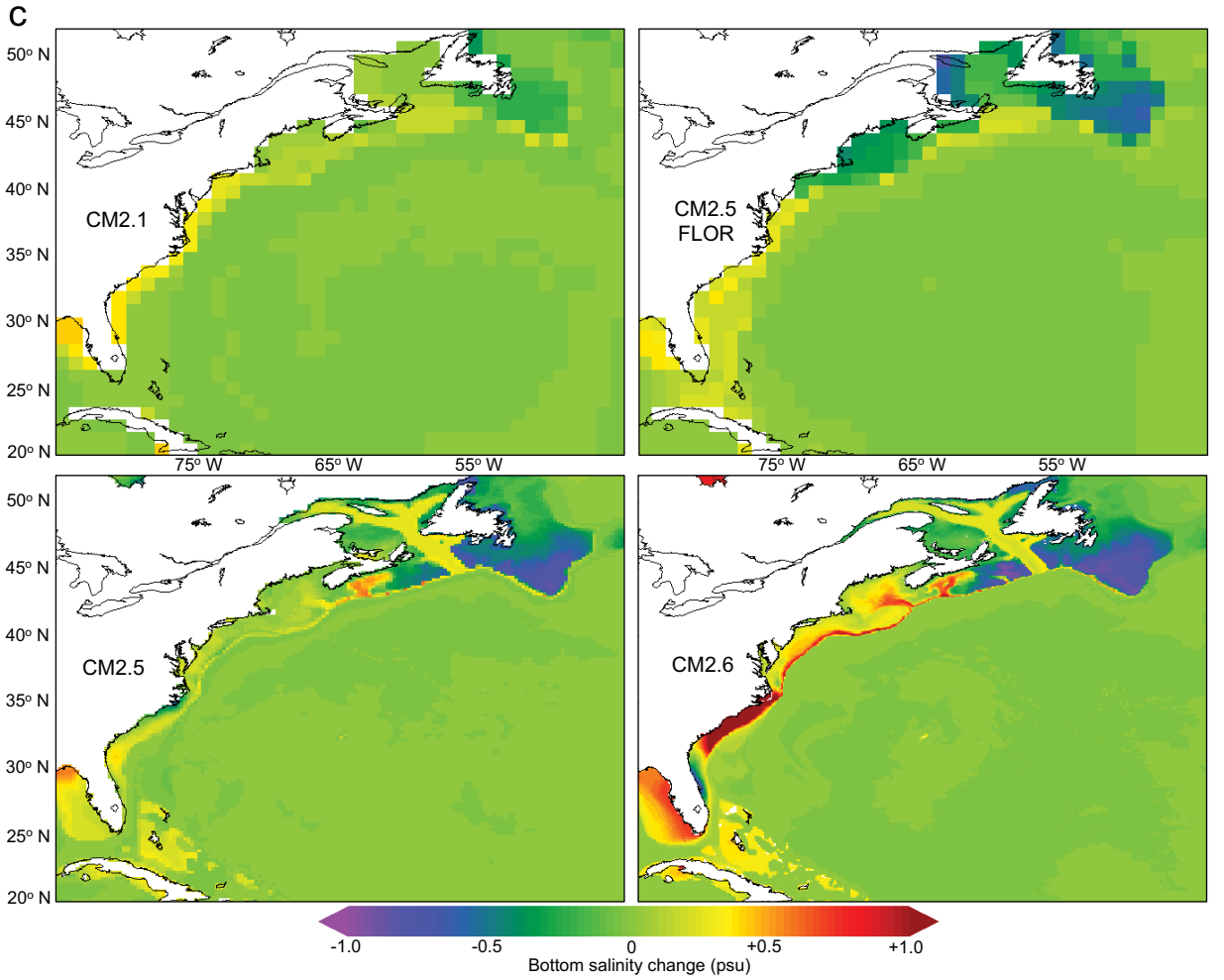

Figure 5. (continued)

the halocline) between coarse and high-resolution climate models, which may be related to differences in each model's eddy responses or mean circulation states. Resolving mesoscale eddies in global climate models might be critical to transient ocean heat uptake both laterally and vertically [*Griffies et al.*, 2015].

Examining the ocean change in CM2.6 in more detail, we find an enhanced warming and a more substantial increase in salinity in not only the surface waters of the Northwest Atlantic Ocean but also in the bottom waters of the Northwest Atlantic Shelf (Figures 5a and 5c). The increase in both temperature and salinity is associated with a northerly shift of the Gulf Stream (Figures 6a and 6b), a retreat of the Labrador Current (Figure 6a), and the replacement of cold Labrador Slope Water by warm Atlantic Temperate Slope Water along the Shelf Slope (Figures 7a–7c; supporting information Movie S1). This water mass replacement leads to a higher proportion of warmer and saltier Atlantic Temperate Slope Water entering the Shelf via the Northeast Channel (Figures 5a, 5c, and 7c).

3.3. Associations to AMOC

The North Atlantic Ocean is a region where changes in AMOC should be most pronounced via changes in sea surface temperature and salinity [*Stouffer et al.*, 2006]. Synchronous with a weakening AMOC is a cooling and freshening of the North Atlantic subpolar gyre [*Collins et al.*, 2013; *Stouffer et al.*, 2006; *Rahmstorf et al.*, 2015]. As stated earlier, the magnitude of cooling in the subpolar North Atlantic is proportional to the rate of AMOC weakening under a transient climate response [*Winton et al.*, 2014]. Recent observations and modeling studies in the Northwest Atlantic Ocean point to a robust, inverse relationship between the Atlantic Meridional Overturning Circulation (AMOC) and the position of the Gulf Stream [*Zhang*, 2008]. A weaker AMOC is related to a more northerly position of the Gulf Stream [*Joyce and Zhang*, 2010; *Zhang et al.*, 2011] through the interaction with

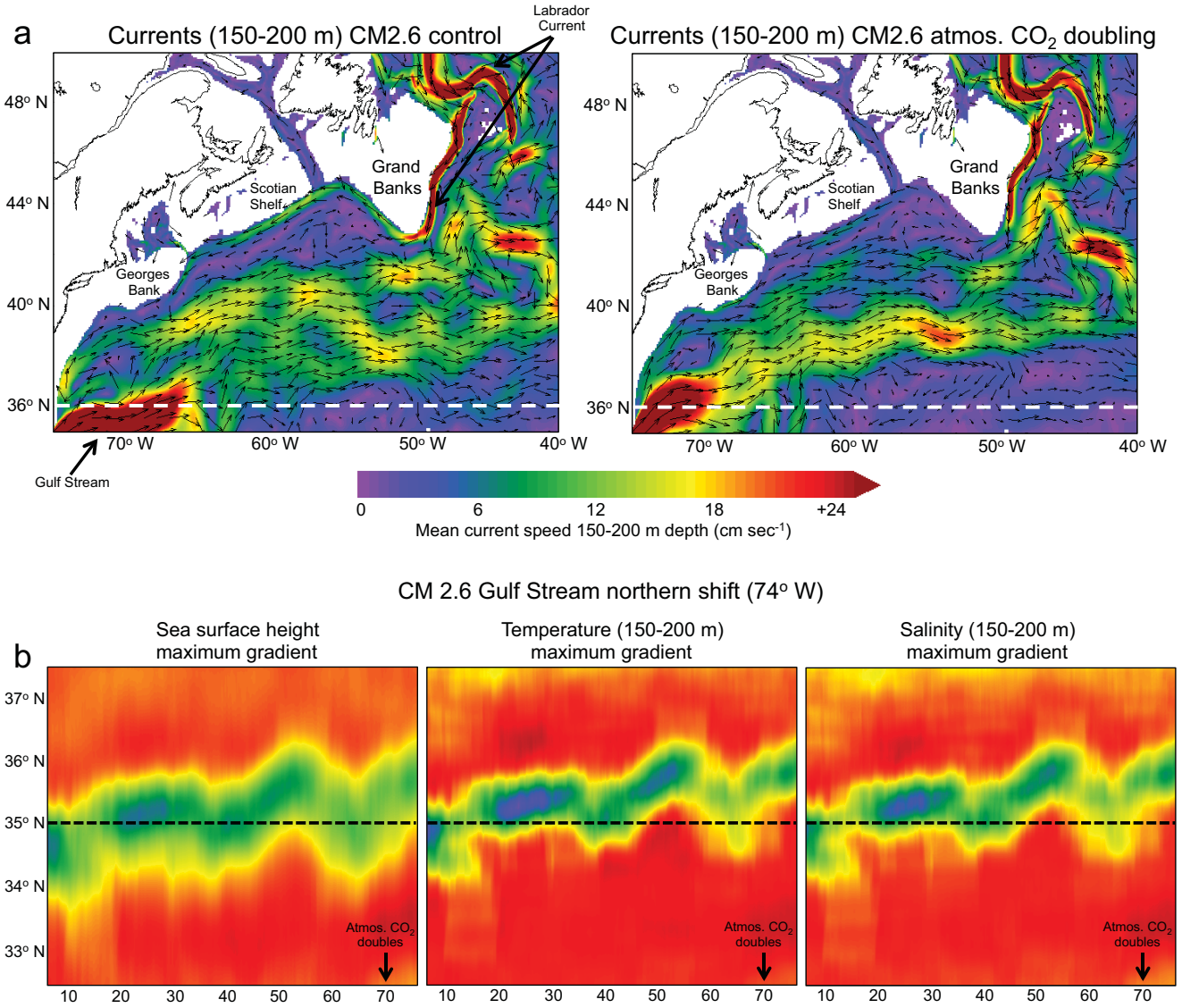

Figure 6. Change in mean ocean currents as a function of speed/direction and change in the Gulf Stream position based on maximum gradients in sea surface height, temperature, and salinity in the Northwest Atlantic after a doubling of global atmospheric CO_2 in CM2.6. (a) Ocean subsurface current speed and direction (150–200 m) from GFDL CM2.6 in the 1860 control run versus 2× CO_2 run (same 20 year mean periods in Figures 4 and 5). The white dashed line marks the 36°N latitude. (b) Change in the latitudinal position of the Gulf Stream determined by maximum gradients of sea surface height, subsurface temperature (150–200 m), and subsurface salinity (150–200 m) at 74°W as atmospheric CO_2 increases 1%/yr and doubles at year 70 (10 year smoothed). The maximum gradient of each variable is calculated by the centered derivative (i.e., change in magnitude per unit distance). The black dashed line marks the 35°N latitude. Red colors represent little to no gradient and yellow, green, blue, and purple represent increasing gradient magnitude.

bottom topography and associated bottom vortex stretching [*Zhang and Vallis*, 2007]. A northerly shift in the Gulf Stream is associated with warmer ocean temperature in the Northwest Atlantic Ocean [*Zhang and Vallis*, 2007]. Therefore, we suggest that the physical mechanism behind the shifts in the Gulf Stream, Labrador Current, and associated water mass replacement along the Northwest Atlantic Shelf is the weakening of AMOC.

The AMOC in CM2.6 weakens by about 3.0 Sv under a CO_2 doubling scenario, which is a greater weakening than in CM2.5 (1.5 Sv) but much less of a weakening than in CM2.5-FLOR (8.7 Sv) and CM2.1 (6.8 Sv) [*Winton et al.*, 2014]. These differences have been attributed to each model's initial strength in AMOC such that those models with an initially weaker AMOC have less of a weakening under climate change [*Winton et al.*, 2014]. We surmise that the warming (cooling) of the Northwest Atlantic (subpolar North Atlantic) in CM2.6 is greater than in CM2.5 because AMOC weakens in CM2.6 twice as much as it does in CM2.5.

In coarse climate models such as CM2.1, the North Atlantic Straights are widened in order to weaken the influence of dense water outflows and thus results in a stronger AMOC [*Winton et al.*, 2014] and a reduced bias in the

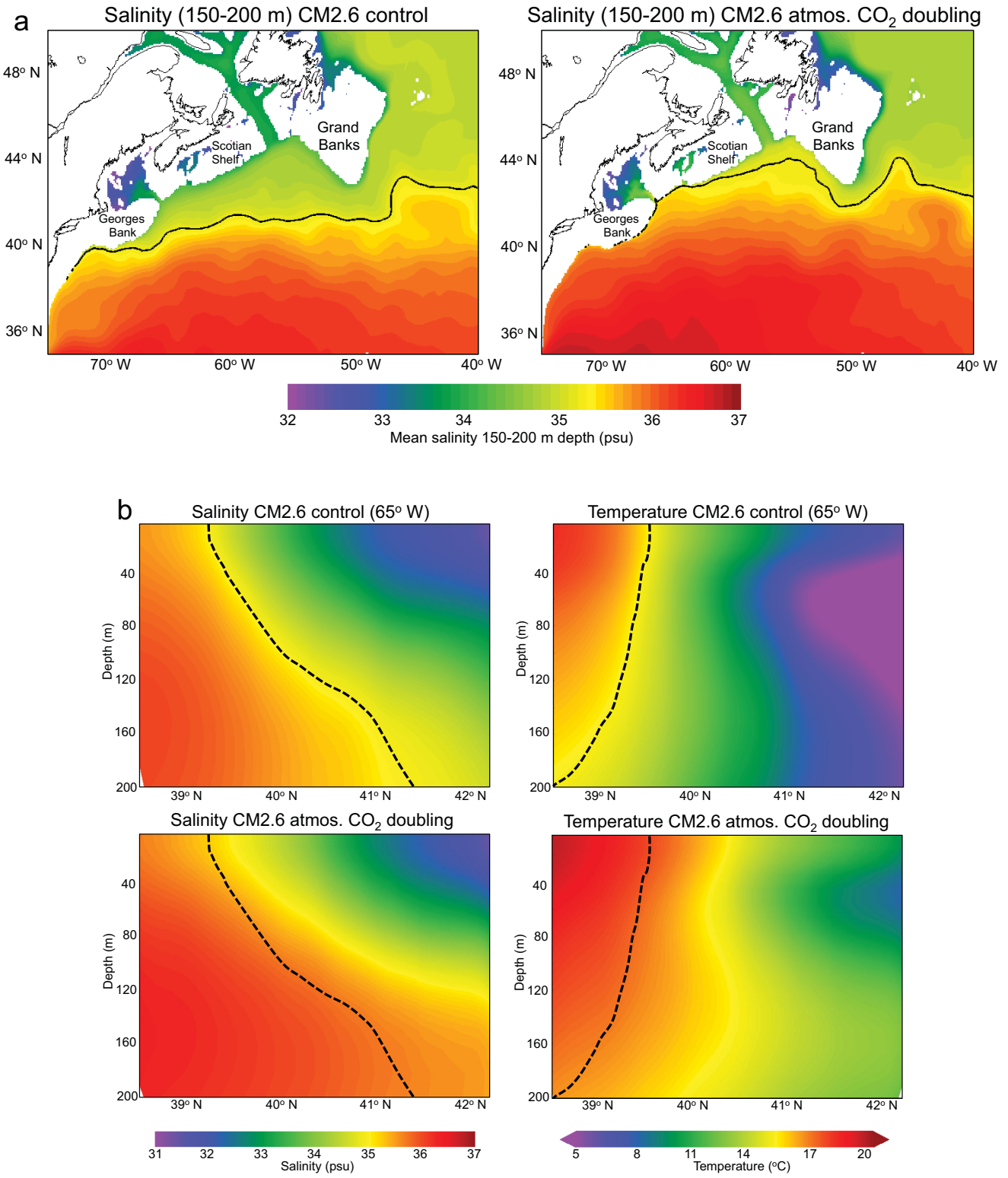

Figure 7. Change in mean temperature and salinity after a doubling of global atmospheric CO_2 in CM2.6 (a) salinity (150–200 m) and the solid black contour line in (a) marks the 35.2 psu halocline. (b) Salinity and temperature profiles at 65°W (Gulf Stream position) between the same CM2.6 runs. The dashed curves in Figure 7b mark the latitudinal positions of the (left) 35 psu halocline and (right) 15°C thermocline in the 1860 control simulation. (c) Change in salinity and temperature at 65°W (top—Gulf Stream position) and at 42.2°N (bottom—Gulf of Maine and Northeast Channel). The Northeast Channel is marked as NEC in Figure 7c. The meridional (65°W) and zonal transects (42.2°N) of these profiles are shown as red dashed lines in Figure 1.

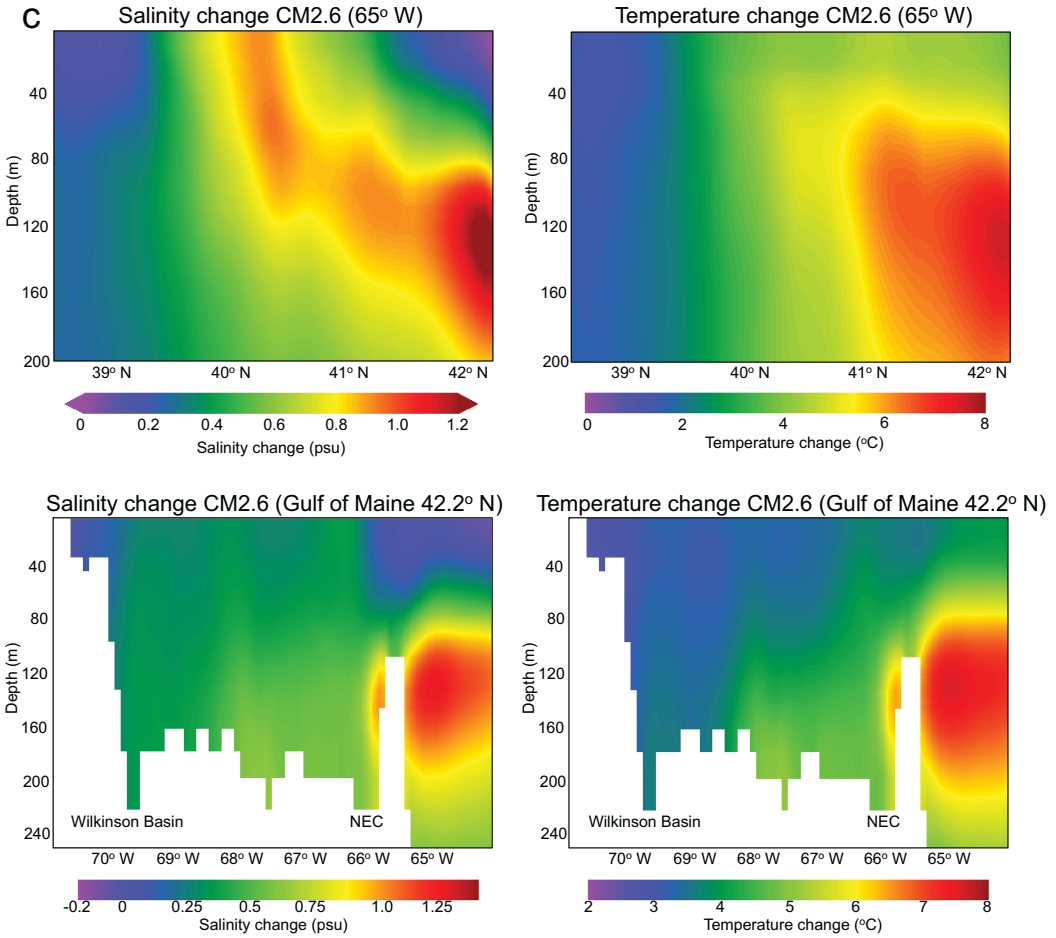

Figure 7. (continued)

position of the North Atlantic Current [*Zhang et al.*, 2011] compared to higher-resolution models. The AMOC at 26.5°N in the 1990 control run of CM2.1 is 18.1 Sv [*Delworth et al.*, 2012], which is much closer to the most recent RAPID observations from 2004 to 2012 (17.2 Sv) [*McCarthy et al.*, 2015] than GFDL's higher-resolution climate models [*Winton et al.*, 2014]. Under the IPCC RCP8.5 highest-emissions scenario, an ensemble of CMIP5 Earth System Models shows that AMOC is projected to weaken by about 6.0 Sv by the year 2100 [*Collins et al.*, 2013]. Therefore, the AMOC weakening in CM2.6 may be too small and thus any additional weakening may lead to an even greater warming and salinity increase in the Northwest Atlantic Ocean and Shelf.

Observations of the interannual variability of AMOC at 26.5°N and Slope Water intrusions in the Northeast Channel (42.25°N) are significantly correlated when AMOC is lagged 1–2 years (Figure 8). A similar correlation is also reported between observations of sea surface height (lagged 2 years) and ocean temperature in the Middle-Atlantic Bight [*Forsyth et al.*, 2015] with a potential link to AMOC such that increased sea level height in the Shelf may be related to a downturn of AMOC [*Goddard et al.*, 2015]. Further evidence for this mechanism arises from the inverse relationship between modeled AMOC measured at 26.5°N and modeled Slope Water intrusions in the Northeast Channel in the 1860 control simulation of CM2.6 (Figure 9). Consequently, weakening of AMOC at 26.5°N in the CM2.6 atmospheric CO_2 doubling experiment leads to an increase in the proportion of warm and salty Slope Water entering the Gulf of Maine's Northeast Channel (Figure 9). A recent study by *Sanchez-Franks and Zhang* [2015] found that an AMOC fingerprint was anticorrelated to the Gulf Stream Path from 1955 to 2014. Although the short time series (2004–2014) of AMOC and the Gulf Stream Path in Figure 8 are not significantly anticorrelated, the longer time series (1955–2014) reported in *Sanchez-Franks and Zhang* [2015] was statistically significant with no lag based on a 5 year moving average. Finally, although a large proportion of observed AMOC interannual variability can be attributed to wind forcing [*Zhao and Johns*, 2014], the weakening of AMOC

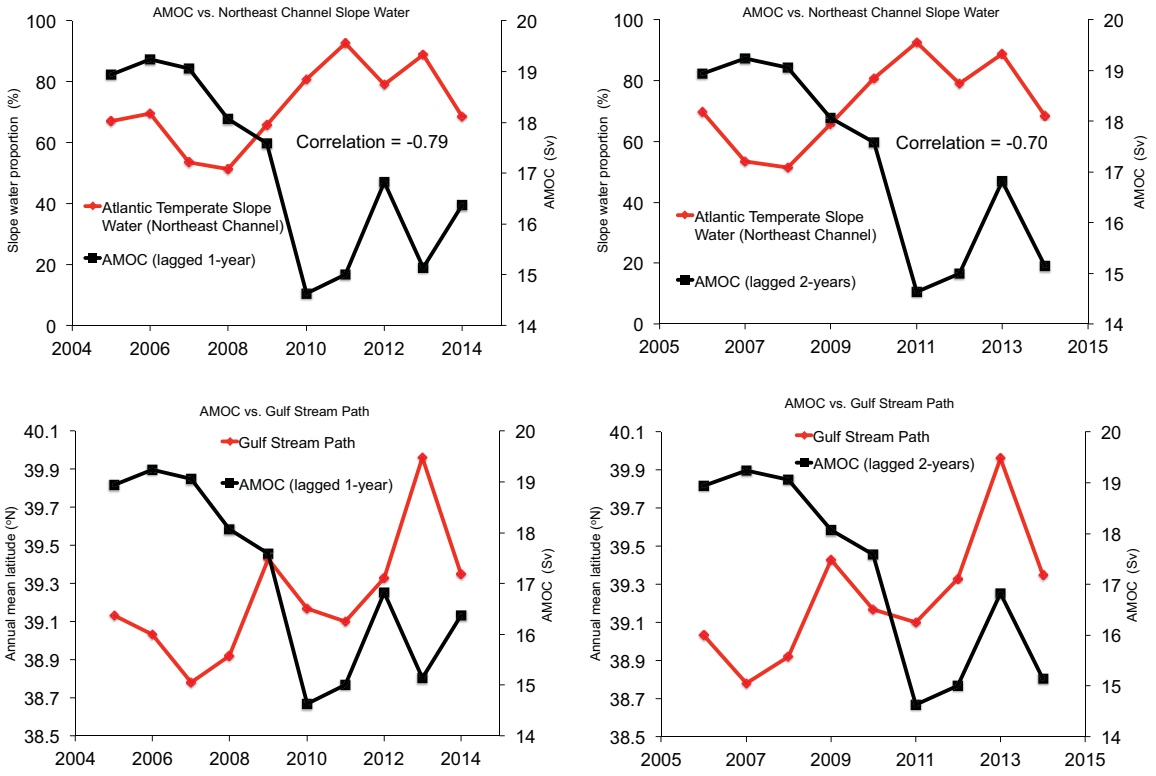

Figure 8. Observed annual AMOC versus Atlantic Temperate Slope Water proportions in the Northeast Channel and the Gulf Stream Path. Annual AMOC values derived from the RAPID-MOC array located across the Atlantic Ocean at 26.5°N. Higher AMOC values indicate more upper-ocean and mid-ocean transport to the North. Annual proportions of Atlantic Temperate Slope Water within the Northeast Channel derived from monthly temperature and salinity measurements within the Channel at depths between 150 and 200 m. Annual positions of the Gulf Stream Path derive from the average latitude of the 15°C isotherm at 200 m from 75°W to 55°W using Levitus data. The annual AMOC is lagged 1 and 2 years prior to each annual value of the Atlantic Temperate Slope Water in the Northeast Channel and each annual value of the Gulf Stream Path (i.e., 2009 = AMOC from 2007 to 2008). Only correlation values that are statistically significant ($P < 0.05$) at the 95% confidence interval are reported.

in response to increasing atmospheric CO_2 in climate models is predominantly caused by changes in surface heat flux relative to changes in surface water flux [*Gregory et al.*, 2005].

4. Summary

In GFDL's CM2.6, the synergy of global warming, the Gulf Stream northerly shift, the Labrador Current retreat, and the increased proportion of Atlantic Temperate Slope Water entering the Shelf cause the enhanced warming of the Northwest Atlantic Ocean and Shelf under a doubling of atmospheric CO_2. In CM2.1 and the majority of coarse climate models assessed by the IPCC, the Gulf Stream coastal separation from the United States in historical simulations is too far to the north of Cape Hatteras and essentially results in a Gulf Stream than flows directly over most of the U.S. Northeast Continental Shelf. Moreover, the detailed bathymetry (i.e., Northeast Channel) that allows for deeper Slope Water intrusions into the Shelf cannot be resolved in a climate model with a coarse (~100 km) ocean component. Therefore, a northern shift in the Gulf Stream in a coarse climate model cannot result in increased Slope Water associated with the Gulf Stream (Atlantic Temperate Slope Water) to enter the Shelf due to its lack of deep channels, which provide a throughway. Moreover, the Northwestern Wall of the Gulf Stream in these coarse models is so close against the U.S. coastline north of Cape Hatteras that there is not much space allowed for a northwestern shift. As discussed in the previous section, the small change in CM2.5's AMOC under an atmospheric CO_2 doubling [*Winton et al.*, 2014] is likely the reason why the warming in the Northwest Atlantic Ocean and Shelf is not as high as it is in CM2.6. Moreover, CM2.6's ocean component is a ~10 km horizontal resolution and appears to resolve Northwest Atlantic Shelf regional circulation more accurately than CM2.5 (~25 km ocean).

Confidence in the transient climate response of CM2.6 for the Northwest Atlantic is driven by the model's ability to resolve both its regional circulation (i.e., position of the Gulf Stream) and fine-scale bathymetry (i.e., Northeast Channel). Additional confidence derives from the skillful simulation of the ocean heat budget

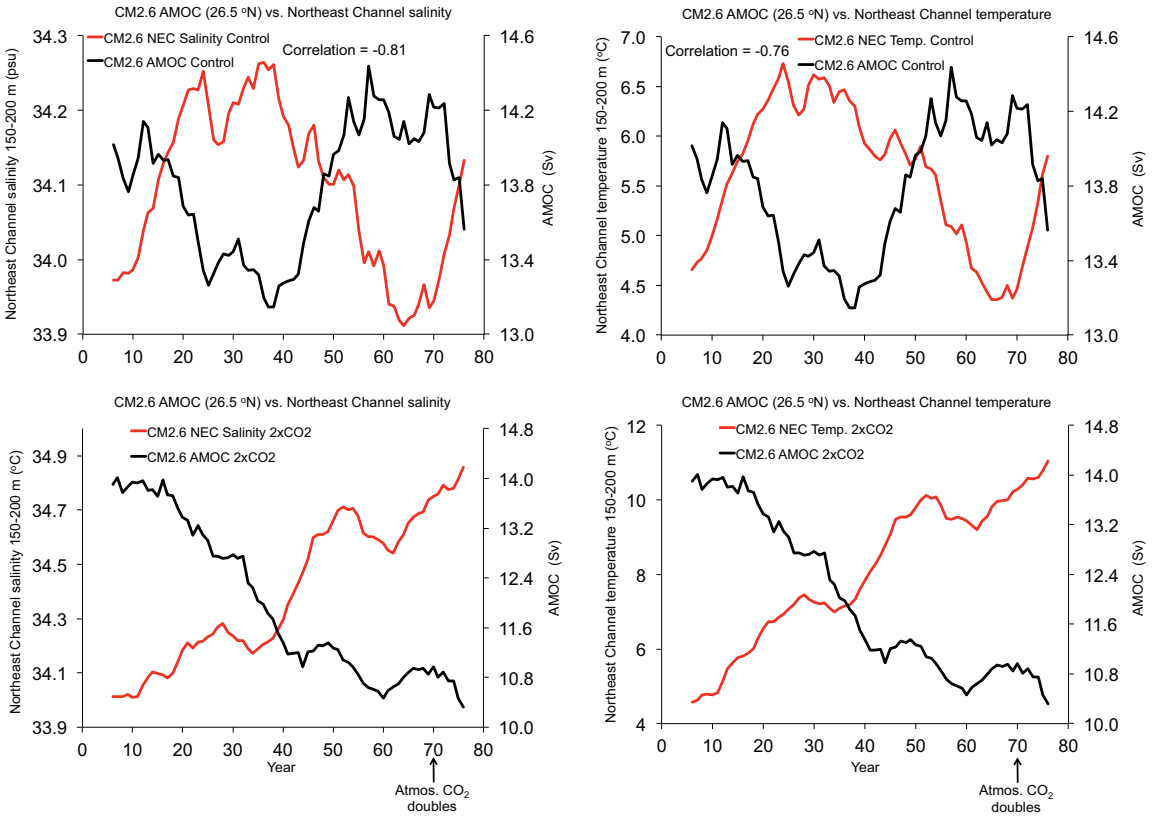

Figure 9. Modeled AMOC versus modeled salinity and temperature in the Northeast Channel from GFDL CM2.6 in the control run and in the CO_2 doubling experiment. The AMOC output from CM2.6 is based on the same metrics as the RAPID-MOC Array at 26.5°N. Salinity and temperature are averaged between 150 and 200 m within the Northeast Channel in CM2.6 to indicate Slope Water intrusions into the Shelf. The model output comes from the 1860 control simulation (80 years) and the CO_2 doubling experiment (80 years). Each time series is a 10 year moving average. Correlation values are statistically significant at the 95% confidence interval.

in CM2.6 relative to CM2.1 and CM2.5 as described in *Griffies et al*. [2015]. This is based on the assumption that the mesoscale ocean resolution in CM2.6 simulates the ocean heat budget more accurately (i.e., smaller temperature drift) compared to coarser models that rely on parameterizing mesoscale features [*Griffies et al*., 2015]. However, CM2.6's cold bias in the North Atlantic Current region along with its relatively weak AMOC (compared to observations) may be partially biasing its transient climate response (atmospheric CO_2 doubling) [*Winton et al*., 2014]. Although the direction of this bias remains unclear, we can only surmise that a stronger AMOC in CM2.6 would lead to a greater AMOC weakening in a transient climate response.

Presently, there are very few global climate models with a high-resolution ocean (∼10 km) because they are cost prohibitive. Another global climate model with a ∼10 km ocean component shows some improvement in the path of the Gulf Stream but the separation from the U.S. coast is still too far to the north of Cape Hatteras [*Small et al*., 2014] and thus regional Northwest Atlantic circulation is not resolved as it is in GFDL's CM2.6. To create ensembles and realize high-resolution model uncertainty, we encourage the continued development of these high-resolution global climate models that include climate change projections.

Enhanced warming of the Northwest Atlantic Ocean and Shelf will have major consequences for the marine ecosystem. Over the past 10 years, the Gulf of Maine has warmed at a rate faster than 99% of the global ocean [*Pershing et al*., 2015]. This enhanced warming of the Gulf of Maine is associated with a northerly shift in the Gulf Stream [*Pershing et al*., 2015], which is similar to our results reported here for GFDL's CM2.6. Contemporary changes in the distribution and species composition of Northwest Atlantic living marine resources [*Nye et al*., 2009; *Pinsky et al*., 2013] are already evident, but existing projections [*Fogarty et al*., 2007; *Hare et al*., 2012; *Lynch et al*., 2015] are based on warming scenarios from coarse resolution models. Warming on the scale of 3–4°C, as shown in GFDL's high-resolution climate model, will cause more extreme effects on the ecosystem.

Acknowledgments
We thank Ron Stouffer and John Dunne for reviewing a previous version of this paper. We also thank the many GFDL personnel that invested time and resources into the development of the climate models evaluated in this research. Ferret (NOAA PMEL) was used to analyze the climate models. We thank Remik Ziemlinski for creating the animation in supporting information Movie S1. In situ data used in this analysis are publically available at the following websites: http://www.bio.gc.ca/science/data-donnees/archive/tsc/scotia/ssmap-en.php, http://www.gebco.net/data_and_products/gridded_bathymetry_data/gebco_30_second_grid, http://www.ncdc.noaa.gov/oisst/data-access, and http://www.rapid.ac.uk/rapidmoc.

References

Bryan, F. O., M. W. Hecht, and R. D. Smith (2007), Resolution convergence and sensitivity studies with North Atlantic circulation models. Part I: The western boundary current system, *Ocean Modell.*, *16*, 141–159, doi:10.1016/j.ocemod.2006.08.005.

Collins, M., et al. (2013), Long-term climate change: Projections, commitments and irreversibility, in *Climate Change 2013: The Physical Science Basis. Contribution of Working Group I to the Fifth Assessment Report of the Intergovernmental Panel on Climate Change*, edited by T. F. Stocker et al., pp. 1029–1136, Cambridge Univ. Press, Cambridge, U. K., doi:10.1017/CBO9781107415324.024.

Delworth, T. L., et al. (2006), GFDL's CM2 global coupled climate models. Part I: Formulation and simulation characteristics, *J. Clim.*, *19*, 643–674.

Delworth, T. L., et al. (2012), Simulated climate and climate change in the GFDL CM2.5 high-resolution coupled climate model, *J. Clim.*, *25*, 2755–2781, doi:10.1175/jcli-d-11-00316.1.

Dengg, J., A. Beckmann, and R. Gerdes (1996), The gulf stream separation problem, in *The Warmwatersphere of the North Atlantic Ocean*, edited by W. Krauss, pp. 253–290, Gebruder-Borntraeger, Stuttgart, Germany.

Flato, G., et al. (2013), Evaluation of climate models, in *Climate Change 2013: The Physical Science Basis. Contribution of Working Group I to the Fifth Assessment Report of the Intergovernmental Panel on Climate Change*, edited by T. F. Stocker et al., pp. 741–866, Cambridge Univ. Press, Cambridge, U. K., doi:10.1017/CBO9781107415324.020.

Fogarty, M., L. Incze, K. Hayhoe, D. Mountain, and J. Manning (2007), Potential climate change impacts on Atlantic cod (*Gadus morhua*) off the northeastern USA, *Mitigation Adaption Strategies Global Change*, *13*(5–6), 453–466, doi:10.1007/s11027-007-9131-4.

Forsyth, J. S. T., M. Andres, and G. G. Gawarkiewicz (2015), Recent accelerated warming of the continental shelf off New Jersey: Observations from the CMVOleander expendable bathythermograph line, *J. Geophys. Res. Oceans*, *120*, 2370–2384, doi:10.1002/2014JC010516.

Goddard, P. B., J. Yin, S. M. Griffies, and S. Zhang (2015), An extreme event of sea-level rise along the Northeast Coast of North America in 2009–2010, *Nat. Commun.*, *6*, 6346, doi:10.1038/ncomms7346.

Gregory, J. M., et al. (2005), A model intercomparison of changes in the Atlantic thermohaline circulation in response to increasing atmospheric CO_2 concentration, *Geophys. Res. Lett.*, *32*, L12703, doi:10.1029/2005GL023209.

Griffies, S. M., et al. (2015), Impacts on ocean heat from transient mesoscale eddies in a hierarchy of climate models, *J. Clim.*, *28*(3), 952–977, doi:10.1175/jcli-d-14-00353.1.

Hare, J. A., et al. (2012), Cusk (*Brosme brosme*) and climate change: Assessing the threat to a candidate marine fish species under the US Endangered Species Act, *ICES J. Mar. Sci.*, *69*(10), 1753–1768, doi:10.1093/icesjms/fss160.

Joyce, T. M., and R. Zhang (2010), On the path of the Gulf Stream and the Atlantic Meridional Overturning Circulation, *J. Clim.*, *23*(11), 3146–3154, doi:10.1175/2010jcli3310.1.

Lynch, P. D., J. A. Nye, J. A. Hare, C. A. Stock, M. A. Alexander, J. D. Scott, K. L. Curti, and K. Drew (2015), Projected ocean warming creates a conservation challenge for river herring populations, *ICES J. Mar. Sci.*, *72*(2), 374–387, doi:10.1093/icesjms/fsu134.

McCarthy, G. D., D. A. Smeed, W. E. Johns, E. Frajka-Williams, B. I. Moat, D. Rayner, M. O. Baringer, C. S. Meinen, J. Collins, and H. L. Bryden (2015), Measuring the Atlantic Meridional Overturning Circulation at 26°N, *Prog. Oceanogr.*, *130*, 91–111, doi:10.1016/j.pocean.2014.10.006.

Mountain, D. G. (2012), Labrador slope water entering the Gulf of Maine—Response to the North Atlantic Oscillation, *Cont. Shelf Res.*, *47*, 150–155, doi:10.1016/j.csr.2012.07.008.

Nye, J. A., J. S. Link, J. A. Hare, and W. J. Overholtz (2009), Changing spatial distribution of fish stocks in relation to climate and population size on the Northeast United States continental shelf, *Mar. Ecol. Prog. Ser.*, *393*, 111–129, doi:10.3354/meps08220.

Pershing, A. J., et al. (2015), Slow adaptation in the face of rapid warming leads to collapse of the Gulf of Maine cod fishery, *Science*, *350*(6262), 809–812, doi:10.1126/science.aac9819.

Pinsky, M. L., B. Worm, M. J. Fogarty, J. L. Sarmiento, and S. A. Levin (2013), Marine taxa track local climate velocities, *Science*, *341*(6151), 1239–1242, doi:10.1126/science.1239352.

Rahmstorf, S., J. E. Box, G. Feulner, M. E. Mann, A. Robinson, S. Rutherford, and E. J. Schaffernicht (2015), Exceptional twentieth-century slowdown in Atlantic Ocean overturning circulation, *Nat. Clim. Change*, *5*, 475–480, doi:10.1038/nclimate2554.

Sanchez-Franks, A., and R. Zhang (2015), Impact of the Atlantic meridional overturning circulation on the decadal variability of the Gulf Stream path and regional chlorophyll and nutrient concentrations, *Geophys. Res. Lett.*, *42*, doi:10.1002/2015GL066262, in press.

Small, R. J., et al. (2014), A new synoptic scale resolving global climate simulation using the Community Earth System Model, *J. Adv. Model. Earth Syst.*, *6*, 1065–1094, doi:10.1002/2014MS000363.

Stock, C. A., M. A. Alexander, N. A. Bond, K. M. Brander, W. W. L. Cheung, E. N. Curchitser, T. L. Delworth, J. P. Dunne, S. M. Griffies, and M. A. Haltuch (2011), On the use of IPCC-class models to assess the impact of climate on Living Marine Resources, *Prog. Oceanogr.*, *88*(1–4), 1–27, doi:10.1016/j.pocean.2010.09.001.

Stouffer, J. Y., et al. (2006), Investigating the causes of the response of the thermohaline circulation to past and future climate changes, *J. Clim.*, *19*, 1365–1387.

Townsend, D. W., A. C. Thomas, L. M. Mayer, M. A. Thomas, and J. A. Quinlan (2006), Oceanography of the Northwest Atlantic Continental Shelf, in *The Sea: The Global Coastal Ocean: Interdisciplinary Regional Studies and Syntheses*, edited by A. R. Robinson and K. H. Brink, pp. 119–168, Harvard Univ. Press, Cambridge, Mass.

Townsend, D. W., N. D. Rebuck, M. A. Thomas, L. Karp-Boss, and R. M. Gettings (2010), A changing nutrient regime in the Gulf of Maine, *Cont. Shelf Res.*, *30*(7), 820–832, doi:10.1016/j.csr.2010.01.019.

Vecchi, G. A., et al. (2014), On the seasonal forecasting of regional tropical cyclone activity, *J. Clim.*, *27*(21), 7994–8016, doi:10.1175/jcli-d-14-00158.1.

Wang, C., L. Zhang, S.-K. Lee, L. Wu, and C. R. Mechoso (2014), A global perspective on CMIP5 climate model biases, *Nat. Clim. Change*, *4*(3), 201–205, doi:10.1038/nclimate2118.

Winton, M., W. G. Anderson, T. L. Delworth, S. M. Griffies, W. J. Hurlin, and A. Rosati (2014), Has coarse ocean resolution biased simulations of transient climate sensitivity?, *Geophys. Res. Lett.*, *41*, 8522–8529, doi:10.1002/2014GL061523.

Zhang, R. (2008), Coherent surface-subsurface fingerprint of the Atlantic meridional overturning circulation, *Geophys. Res. Lett.*, *35*, L20705, doi:10.1029/2008GL035463.

Zhang, R., and G. K. Vallis (2007), The role of bottom vortex stretching on the path of the North Atlantic Western Boundary Current and on the Northern Recirculation Gyre, *J. Phys. Oceanogr.*, *37*(8), 2053–2080, doi:10.1175/jpo3102.1.

Zhang, R., T. L. Delworth, A. Rosati, W. G. Anderson, K. W. Dixon, H.-C. Lee, and F. Zeng (2011), Sensitivity of the North Atlantic Ocean Circulation to an abrupt change in the Nordic Sea overflow in a high resolution global coupled climate model, *J. Geophys. Res.*, *116*, C12024, doi:10.1029/2011JC007240.

Zhao, J., and W. Johns (2014), Wind-forced interannual variability of the Atlantic Meridional Overturning Circulation at 26.5°N, *J. Geophys. Res. Oceans*, *119*, 2403–2419, doi:10.1002/2013JC009407.